

Majorana fermions induced fast- and slow-light in a hybrid semiconducting nanowire/superconductor device

Hua-Jun Chen(陈华俊), Peng-Jie Zhu(朱鹏杰), Yong-Lei Chen(陈咏雷), and Bao-Cheng Hou(侯宝成)

Citation: Chin. Phys. B, 2022, 31 (**2**): 027802. DOI: 10.1088/1674-1056/ac3221
Journal homepage: http://cpb.iphy.ac.cn; http://iopscience.iop.org/cpb

What follows is a list of articles you may be interested in

Photonic-plasmonic hybrid microcavities: Physics and applications

Hongyu Zhang(张红钰), Wen Zhao(赵闻), Yaotian Liu(刘耀天), Jiali Chen(陈佳丽), Xinyue Wang(王欣月), and Cuicui Lu(路翠翠)

Chin. Phys. B, 2021, 30 (**11**): 117801. DOI: 10.1088/1674-1056/ac0db3

Thermally induced band hybridization in bilayer-bilayer MoS_2/WS_2 heterostructure

Yanchong Zhao(赵岩翀), Tao Bo(薄涛), Luojun Du(杜罗军), Jinpeng Tian(田金朋), Xiaomei Li(李晓梅), Kenji Watanabe, Takashi Taniguchi, Rong Yang(杨蓉), Dongxia Shi(时东霞), Sheng Meng(孟胜), Wei Yang(杨威), and Guangyu Zhang(张广宇)

Chin. Phys. B, 2021, 30 (**5**): 057801. DOI: 10.1088/1674-1056/abeee3

Quantum plasmons in the hybrid nanostructures of double vacancy defected graphene and metallic nanoarrays

Rui Tang(唐睿), Yang Xu(徐阳), Hong Zhang(张红), and Xin-Lu Cheng(程新路)

Chin. Phys. B, 2021, 30 (**1**): 017804. DOI: 10.1088/1674-1056/abaedb

Acoustic plasmonics of Au grating/Bi_2Se_3 thin film/sapphirehybrid structures

Weiwu Li(李伟武), Konstantin Riegel, Chuanpu Liu(刘传普), Alexey Taskin, Yoichi Ando, Zhimin Liao(廖志敏), Martin Dressel, Yuan Yan(严缘)

Chin. Phys. B, 2020, 29 (**6**): 067801. DOI: 10.1088/1674-1056/ab8a3c

Control of light scattering by nanoparticles with optically-induced magnetic responses

Liu Wei, Andrey E. Miroshnichenko, Yuri S. Kivshar

Chin. Phys. B, 2014, 23 (**4**): 047806. DOI: 10.1088/1674-1056/23/4/047806

Majorana fermions induced fast- and slow-light in a hybrid semiconducting nanowire/superconductor device

Hua-Jun Chen(陈华俊)†, Peng-Jie Zhu(朱鹏杰), Yong-Lei Chen(陈咏雷), and Bao-Cheng Hou(侯宝成)

School of Mechanics and Photoelectric Physics, Anhui University of Science and Technology, Huainan 232001, *China*

(Received 7 July 2021; revised manuscript received 19 September 2021; accepted manuscript online 22 October 2021)

We investigate theoretically Rabi-like splitting and Fano resonance in absorption spectra of quantum dots (QDs) based on a hybrid QD-semiconducting nanowire/superconductor (SNW/SC) device mediated by Majorana fermions (MFs). Under the condition of pump on-resonance and off-resonance, the absorption spectrum experiences the conversion from Fano resonance to Rabi-like splitting in different parametric regimes. In addition, the Fano resonances are accompanied by the rapid normal phase dispersion, which will indicate the coherent optical propagation. The results indicate that the group velocity index is tunable with controlling the interaction between the QD and MFs, which can reach the conversion between the fast- and slow-light. Fano resonance will be another method to detect MFs and our research may indicate prospective applications in quantum information processing based on the hybrid QD-SNW/SC devices.

Keywords: majorana fermions, Fano resonance, slow and fast light, hybrid semiconducting/superconductor device

PACS: 78.67.Hc, 42.50.–p, 42.50.Gy **DOI:** 10.1088/1674-1056/ac3221

1. Introduction

Majorana fermions (MFs) have witnessed significant progress over the past decade in solid state systems for their potential applications in topological quantum computation and quantum information processing[1–7] due to the fact that they obey non-Abelian statistics. Although MFs were proposed originally as a model for neutrinos, the analogous Majorana zero modes have been observed in condensed matter systems,[8] such as hybrid semiconducting nanowire/superconductor (SNW/SC) structures,[9–12] ferromagnetic atomic chains on a superconductor,[13] iron-based superconductor device,[14] topological superconductor devices,[15,16] and topological insulator structure.[17] In order to observe Majorana-like signatures, several significant experimental schemes have been proposed, including the zero-bias peaks (ZBPs) in tunneling spectroscopy,[9–13] the Josephson effect,[18] the Coulomb blockade spectroscopy,[15] and the spin-resolved measurements.[19]

On the other hand, due to the significant progress in modern nanoscience and nanotechnology, artificial atoms, i.e., quantum dots (QDs),[20–25] manifest the attractive intermediary for probing MFs both theoretically[26–30] and experimentally.[31] However, in the detection of MFs with QDs in the electrical domain, QDs are always considered as only a resonant level.[26–30] Different from the previous schemes for probing MFs, we have presented an optical scheme for probing MFs with a QD considered as a two-level system (TLS) and driven by the optical pump-probe technology,[32–35] which may provide a potential supplement for probing MFs. However, Rabi splitting and Fano resonance induced by MFs in optical domain based on a hybrid QD-SNW/SC device have not yet been explored to the best of our knowledge, needless to say reaching the coherent optical propagation, such as the fast- and slow-light effects.

In this paper, firstly we demonstrate that the probe absorption spectra of the QD show the switch from Rabi-like splitting to Fano resonance induced by MFs for different detuning regimes in the hybrid QD-SNW/SC device, which can be illustrated using the interference effect with the dressed state theory. Under the condition of pump on-resonance, the probe absorption spectra present a distinct Rabi splitting behavior with increasing the QD-MFs coupling strength β, which manifests a strong interaction of the QD and MFs, and the width of the splitting is 2β, which indicates an approach to determine the QD-MFs coupling strength. In the pump off-resonance, the probe absorption spectra can show a series of asymmetric Fano line shapes, and the Fano resonances are tunable under different parametric regimes, such as the Majorana-pump field detuning $\Delta_{\rm M}$ and the exciton-pump field detuning $\Delta_{\rm c}$. As Fano resonances are characterized by a rapid steeper dispersion, the light pulses can be accelerated and decreased significantly, which correspond to the negative and positive dispersions, respectively, and then reach the fast and slow light effect. Secondly, we investigate the coherent optical propagation properties, i.e., the fast and slow light effect via the group delay of the probe field around the transparency window accompanied by the steep phase dispersion. The results show that a controllable fast-to-slow light propagation can be reached with manipulating the parametric regimes.

†Corresponding author. E-mail: chenphysics@126.com

© 2022 Chinese Physical Society and IOP Publishing Ltd

2. Model and method

The system under consideration is sketched in Fig. 1, where a QD coupled to a near by MFs appearing in the hybrid SNW/SC device,[9–12] and the Hamiltonian is given by[26–30,32–35]

$$\begin{aligned} H_1 &= \hbar\omega_{\rm ex}S^z + {\rm i}\varepsilon_{\rm M}\gamma_1\gamma_2/2 + {\rm i}\hbar\beta(S^- - S^+)\gamma_1 \\ &\quad -\mu\varepsilon_{\rm p}(S^+{\rm e}^{-{\rm i}\omega_{\rm p}t} + S^-{\rm e}^{{\rm i}\omega_{\rm p}t}) \\ &\quad -\mu\varepsilon_{\rm s}(S^+{\rm e}^{-{\rm i}\omega_{\rm s}t} + S^-{\rm e}^{{\rm i}\omega_{\rm s}t}), \end{aligned} \tag{1}$$

where the first term indicates the Hamiltonian of the QD with the exciton frequency $\omega_{\rm ex}$. In the previous works for probing MFs, the QD is consider as a single resonant level with spin-singlet state,[26–30] here we consider that the QD is a TLS with the ground state $|0\rangle$ and the single exciton state $|1\rangle$, which is described by the pseudospin operators S^z and $S^\pm$ with the commutation relations $[S^z, S^\pm] = \pm S^\pm$ and $[S^+, S^-] = 2S^z$.

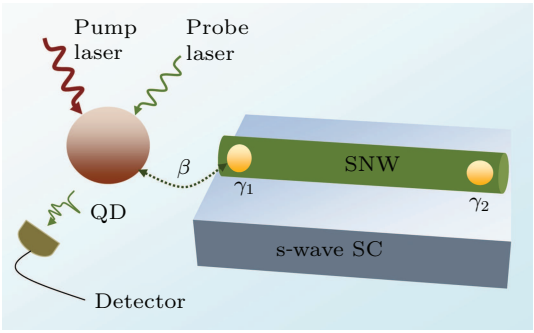


Fig. 1. The schematic of the hybrid QD-SNW/SC device, in which a QD driven by a pump field and a probe field coupled to a nearby MF in the end of SNW.

The second term is the interaction of the two MFs in the end of SNW in the hybrid SNW/SC device. To describe MFs, we introduce the Majorana operators γ_1 and γ_2 with the relation $\gamma^\dagger = \gamma$ and $\gamma^2 = 1$ as they are their own antiparticles. Here, $\varepsilon_{\rm M} = \hbar\omega_{\rm M} \sim {\rm e}^{-l/\xi}$ is the coupling energy with l being the length of the SNW and ξ the superconducting coherent length with Majorana frequency $\omega_{\rm M}$. If the length l of the SNW is large enough, we can find the coupling energy $\varepsilon_{\rm M} \sim {\rm e}^{-l/\xi} \sim 0$. Thus, we need to discuss the two cases, i.e., $\varepsilon_{\rm M} \neq 0$ in terms of coupled Majorana edge states, and $\varepsilon_{\rm M} = 0$ in terms of uncoupled Majorana edge states.

The third gives the nearby MFs γ_1 coupled to the QD with the coupling strength β, and the coupling strength is related to the distance of the QD and SNW/SC device. For simplicity, we introduce the regular fermion creation and annihilation operators $f^\dagger$ and f with the anti-commutative relation $\{f, f^\dagger\} = 1$, thus, according to the relation of $\gamma_1 = f^\dagger + f$ and $\gamma_2 = {\rm i}(f^\dagger - f)$, Majorana operator γ can be transformed into the regular fermion operator f. Then the third term reduces to ${\rm i}\hbar\beta(S^- f^\dagger - S^+ f)$ with neglecting the non-conservation terms of energy ${\rm i}\hbar\beta(S^- f - S^+ f^+)$ based on the rotating wave approximation.[36]

The last two terms indicate the interactions between the QD and two laser fields including a strong pump field with frequency $\omega_{\rm p}$ and a weak probe field with frequency $\omega_{\rm s}$ simultaneously irradiating to the QD, where μ is the electric dipole moment of the exciton, $\varepsilon_{\rm p}$ and $\varepsilon_{\rm s}$ are the slowly varying envelope of the pump field and probe field, respectively. In a frame rotated to the frequency $\omega_{\rm p}$ of the pump field, Eq. (1) can be rewritten as

$$\begin{aligned} H &= \hbar\Delta_{\rm p}S^z + \hbar\Delta_{\rm M}(f^\dagger f - 1/2) \\ &\quad + {\rm i}\hbar\beta(S^- f^\dagger - S^+ f) - \hbar\Omega_{\rm p}(S^+ + S^-) \\ &\quad -\mu\varepsilon_{\rm s}(S^+{\rm e}^{-{\rm i}\delta t} + S^-{\rm e}^{{\rm i}\delta t}), \end{aligned} \tag{2}$$

where $\Delta_{\rm p} = \omega_{\rm ex} - \omega_{\rm p}$ indicates the exciton-pump field detuning, $\Delta_{\rm M} = \omega_{\rm M} - \omega_{\rm p}$ means the Majorana-pump field detuning, and $\delta = \omega_{\rm s} - \omega_{\rm p}$ gives the probe-pump detuning. Here, $\Omega_{\rm p} = \mu\varepsilon_{\rm p}/\hbar$ is the Rabi frequency of the pump field. According to the Heisenberg equation of motion ${\rm i}\hbar\partial\rho/\partial t = [\rho, H]$ ($\rho = S^z, S^-, f$), we can obtain the Heisenberg–Langevin equations of the operators with the corresponding noise and damping terms as follows:

$$\begin{aligned} \dot{S}^z &= -\Gamma_1(S^z + 1/2) - \beta(S^- f^\dagger + S^+ f) + {\rm i}\Omega_{\rm p}(S^+ - S^-) \\ &\quad + ({\rm i}\mu\varepsilon_{\rm s}/\hbar)(S^+{\rm e}^{-{\rm i}\delta t} - S^-{\rm e}^{{\rm i}\delta t}), \end{aligned} \tag{3}$$

$$\begin{aligned} \dot{S}^- &= -({\rm i}\Delta_{\rm p} + \Gamma_2)S^- + 2\beta S^z f \\ &\quad - 2{\rm i}\Omega_{\rm p}S^z - 2{\rm i}\mu\varepsilon_{\rm s}S^z{\rm e}^{-{\rm i}\delta t}/\hbar + \hat{F}_{\rm in}(t), \end{aligned} \tag{4}$$

$$\dot{f} = -({\rm i}\Delta_{\rm M} + \kappa_{\rm M}/2)f + \beta S^- + \hat{\xi}(t), \tag{5}$$

where Γ_1 (Γ_2) is the exciton relaxation rate (exciton dephasing rate), and $\kappa_{\rm M}$ is the decay rate of the MFs. $\hat{F}_{\rm in}(t)$ is the δ-correlated Langevin noise operator with zero mean, and ξ is Langevin force arising from the interaction between the Majorana modes and the environment.

We introduce the perturbation theory: $\rho = \rho_0 + \delta\rho$, where ρ indicates the operators S^z, S^-, and f, then ρ_0 (i.e., S_0^z, S_0, and f_0) means the steady parts, and $\delta\rho$ (i.e., δS^z, δS^-, and δf) indicates the fluctuation ones. Substituting the perturbation method into Eqs. (3)–(5) we obtain the steady state solutions of the variables as follows:

$$\Gamma_1(w_0 + 1) + 2\beta(S_0 f_0^* + S_0^* f_0) = 2{\rm i}\Omega_{\rm p}(S_0 - S_0^*), \tag{6}$$

$$\beta f_0 w_0 - ({\rm i}\Delta_{\rm p} + \Gamma_2)S_0 = {\rm i}\Omega_{\rm p} w_0, \tag{7}$$

$$({\rm i}\Delta_{\rm M} + \kappa_{\rm M}/2)f_0 - \beta S_0 = 0, \tag{8}$$

which determine the steady-state population inversion ($w_0 = 2S_0^z$) of the exciton as follows:

$$\begin{aligned} &\Gamma_1(w_0 + 1)(\Xi_1^2 + \Gamma_2^2\Xi_2 + \Xi_3) \\ &-4\beta^2\Omega_{\rm p}^2\kappa_{\rm M}w_0^2 + 4\Omega_{\rm p}^2 w_0\Gamma_2\Xi_2 = 0, \end{aligned} \tag{9}$$

where $\Xi_1 = \beta^2 w_0 + \Delta_{\rm p}\Delta_{\rm M}$, $\Xi_2 = \Delta_{\rm M}^2 + \kappa_{\rm M}^2/4$, and $\Xi_3 = \Delta_{\rm p}^2\kappa_{\rm M}^2/4 - \beta^2\Gamma_2\kappa_{\rm M}w_0$. As all the pump fields are assumed to be sufficiently strong, all the operators can be identified with

their expectation values under the mean-field approximation $\langle Qc\rangle = \langle Q\rangle\langle c\rangle$,[37] after being linearized by neglecting nonlinear terms in the fluctuations, the H-LEs for the expectation values are

$$\begin{aligned}\langle\delta\dot{S}^z\rangle &= -\Gamma_1\langle\delta S^z\rangle - \beta(S_0\langle\delta f^\dagger\rangle + S_0^*\langle\delta f\rangle \\ &\quad + f_0^*\langle\delta S^-\rangle + f_0\langle\delta S^+\rangle) + \mathrm{i}\Omega_\mathrm{p}(\langle\delta S^+\rangle - \langle\delta S^-\rangle) \\ &\quad + \frac{\mathrm{i}\mu\varepsilon_\mathrm{s}}{\hbar}(S_0^*\mathrm{e}^{-\mathrm{i}\delta t} - S_0\mathrm{e}^{\mathrm{i}\delta t}), \qquad (10)\\ \langle\delta\dot{S}^-\rangle &= -(\mathrm{i}\Delta_\mathrm{p} + \Gamma_2)\langle\delta S\rangle + \beta w_0\langle\delta f\rangle \\ &\quad + (2\beta f_0 - \mathrm{i}\Omega_\mathrm{p})\langle\delta S^z\rangle - \frac{\mathrm{i}\mu\varepsilon_\mathrm{s}w_0\mathrm{e}^{-\mathrm{i}\delta t}}{\hbar}, \qquad (11)\\ \langle\delta\dot{f}\rangle &= -(\mathrm{i}\Delta_\mathrm{M} + \kappa_\mathrm{M}/2)\langle\delta f\rangle + \beta\langle\delta S^-\rangle. \qquad (12)\end{aligned}$$

In order to solve the equation set of the above H-LEs, we make the ansatz[38] $\langle\delta\rho\rangle = \rho_+\mathrm{e}^{-\mathrm{i}\delta t} + \rho_-\mathrm{e}^{\mathrm{i}\delta t}$. Solving the equation set and working to the lowest order in ε_s but to all orders in ε_p, we obtain the linear optical susceptibility as $\chi_\mathrm{eff}^{(1)}(\omega_\mathrm{s}) = \mu S_+(\omega_\mathrm{s})/\varepsilon_\mathrm{s} = \Sigma_1\chi^{(1)}(\omega_\mathrm{s})$ with $\Sigma_1 = \mu^2/(\hbar\Gamma_2)$, and then the dimensionless linear susceptibility $\chi^{(1)}(\omega_\mathrm{s})$ is given by

$$\chi^{(1)}(\omega_\mathrm{s}) = \frac{\mathrm{i}[\Pi S_0^* - w_0(\Gamma_1 + \Theta_2\Pi^*/D_2 - \mathrm{i}\delta)]\Gamma_2}{D_1(\Gamma_1 + \Theta_2\Pi^*/D_2 - \mathrm{i}\delta) - \Pi\Theta_1}, \qquad (13)$$

where $\phi_1 = \beta/[\kappa_\mathrm{M}/2 + \mathrm{i}(\Delta_\mathrm{M} - \delta)]$, $\phi_2 = \beta/[\kappa_\mathrm{M}/2 + \mathrm{i}(\Delta_\mathrm{M} + \delta)]$, $\Theta_1 = \mathrm{i}\Omega_\mathrm{p} - \beta(f_0^* + S_0^*\phi_1)$, $\Theta_2 = \mathrm{i}\Omega_\mathrm{p} + \beta(f_0 + S_0\phi_2^*)$, $\Pi = 2(\beta f_0 - \mathrm{i}\Omega_\mathrm{p})$, $D_1 = \Gamma_2 - \beta w_0\phi_1 + \mathrm{i}(\Delta_\mathrm{p} - \delta)$, and $D_2 = \Gamma_2 - \beta w_0\phi_2^* - \mathrm{i}(\Delta_\mathrm{p} + \delta)$. The imaginary and real parts of $\chi^{(1)}(\omega_\mathrm{s})$ indicate absorption and dispersion, respectively.

According to the light group velocity[39,40] $v_\mathrm{g} = c/[n + \omega_\mathrm{s}(\mathrm{d}n/\mathrm{d}\omega_\mathrm{s})]$, where $n \approx 1 + 2\pi\chi_\mathrm{eff}^{(1)}$, we obtain

$$\begin{aligned}\frac{c}{v_\mathrm{g}} &= 1 + 2\pi\,\mathrm{Re}[\chi_\mathrm{eff}^{(1)}(\omega_\mathrm{s})]_{\omega_\mathrm{s}=\omega_\mathrm{ex}} \\ &\quad + 2\pi\omega_\mathrm{s}\,\mathrm{Re}(\mathrm{d}\chi_\mathrm{eff}^{(1)}/\mathrm{d}\omega_\mathrm{s})_{\omega_\mathrm{s}=\omega_\mathrm{ex}}. \qquad (14)\end{aligned}$$

Obviously, when $\mathrm{Re}[\chi_\mathrm{eff}^{(1)}(\omega_\mathrm{s})]_{\omega_\mathrm{s}=\omega_\mathrm{ex}} = 0$, the dispersion is steeply positive or negative, and the group velocity is significantly reduced or increased. We further define the group velocity index n_g as

$$\begin{aligned}n_\mathrm{g} &= \frac{c}{v_\mathrm{g}} - 1 = \frac{c - v_\mathrm{g}}{v_\mathrm{g}} = \frac{2\pi\omega_\mathrm{ex}\rho\mu^2}{\hbar\Gamma_2}\mathrm{Re}\left(\frac{\mathrm{d}\chi_\mathrm{eff}^{(1)}}{\mathrm{d}\omega_\mathrm{s}}\right)_{\omega_\mathrm{s}=\omega_\mathrm{ex}} \\ &= \Gamma_2\Sigma\,\mathrm{Re}\left(\frac{\mathrm{d}\chi_\mathrm{eff}^{(1)}}{\mathrm{d}\omega_\mathrm{s}}\right)_{\omega_\mathrm{s}=\omega_\mathrm{ex}}, \qquad (15)\end{aligned}$$

where $\Sigma = 2\pi\omega_\mathrm{ex}\rho\mu^2/\hbar\Gamma_2^2$. One can observe the slow light if $n_\mathrm{g} > 0$, and the superluminal light when $n_\mathrm{g} < 0$.[41] The parameter values used in the paper:[9–12,35,42] the QD-MFs coupling strength $\beta = 0.1$ GHz, the decay rate of the MFs $\kappa_\mathrm{M} = 0.1$ MHz, $\Gamma_1 = 0.3$ GHz, $\Gamma_2 = 0.15$ GHz, and $\Omega_\mathrm{p}^2 = 0.005$ (GHz)^2.

3. Results and discussion

Firstly, we discuss the case of uncoupled Majorana edge state, i.e., $\varepsilon_\mathrm{M} = 0$ (or $\Delta_\mathrm{M} = 0$) under the condition of the exciton-pump field detuning $\Delta_\mathrm{p} = 0$, and the Hamiltonian describing the coupling between the QD and nearby MFs reduces to $H_\mathrm{int} = \mathrm{i}\hbar\beta(S^-f^\dagger - S^+f)$. Then the absorption spectra will display the symmetric splitting due to the fact that the coupled Hamiltonian is analogical to the J–C Hamiltonian of the standard model. In Fig. 2, we plot the probe absorption (the imaginary part of the dimensionless susceptibility i.e., $\mathrm{Im}\,\chi^{(1)}$) versus the probe-exciton detuning $\Delta_\mathrm{s} = \omega_\mathrm{s} - \omega_\mathrm{ex}$ for several different MF-QD coupling strengths β. Obviously, in the case of $\beta = 0$, i.e., without MF-QD coupling, the absorption spectrum shows a lorentz peak. However, when the MF-QD coupling β is considered, the absorption spectra display an evident splitting behavior, and the splitting is enhanced prominently with increasing the MF-QD coupling β from $\beta = 0.1$ GHz to $\beta = 0.6$ GHz. In addition, the splitting in the absorption spectrum is symmetric, which is like the vacuum Rabi splitting, and the width of splitting is 2β, and the peak splitting manifests the strong interaction between MF and QD. The physical origin of the results comes from the coherent interaction of the QD and MFs, and we introduce the dressed state theory to explain this physical phenomena.[35] Because QD is considered as TLS with the ground state $|0\rangle$ and exciton state $|1\rangle$, when QD is coupled to the nearby MFs, QD will be modified by the number states of the MFs n_M inducing the Majorana dressed states $|0,n_\mathrm{M}\rangle$, $|0,n_\mathrm{M}+1\rangle$, $|1,n_\mathrm{M}\rangle$, $|1,n_\mathrm{M}+1\rangle$. The left sharp peak of splitting in the absorption spectra indicates the transition from $|0\rangle$ to $|1,n_\mathrm{M}\rangle$, and the right sharp peak is due to the transition of $|0\rangle$ to $|1,n_\mathrm{M}+1\rangle$. On the other hand, we find that the absorption dip will reach zero at $\Delta_\mathrm{s} = 0$ when $\beta \neq 0$, that is to say, the input probe field is transmitted completely without any absorption, which is very similar to electromagnetically induced transparency (EIT)[43] in Λ-type atoms systems. Since EIT can induce slow light, the hybrid QD-SWN/SC system can also reach slow light effect.

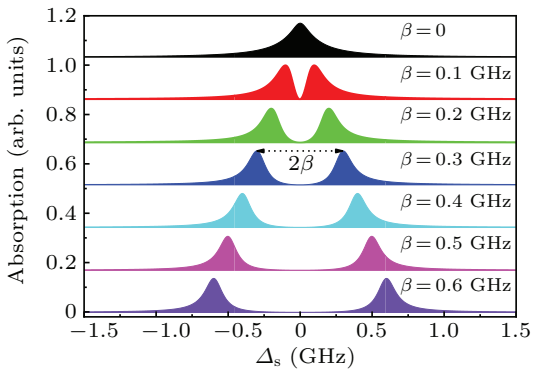


Fig. 2. The probe absorption versus the probe-exciton detuning $\Delta_\mathrm{s} = \omega_\mathrm{s} - \omega_\mathrm{ex}$ for several different MF-QD coupling strengths β. The other parameters are $\Gamma_1 = 0.3$ GHz, $\Gamma_2 = 0.15$ GHz, $\kappa_\mathrm{M} = 0.1$ MHz, $\Omega_\mathrm{p}^2 = 0.005$ (GHz)^2, $\Delta_\mathrm{M} = \Delta_\mathrm{p} = 0$.

In Fig. 3(a), we investigate the dispersion (the real part of the dimensionless susceptibility, i.e., $\mathrm{Re}\,\chi^{(1)}$) as a function of Δ_s for several different MF-QD coupling strengths β at $\Delta_p = 0$. It is obvious that the dispersion exhibits the negative steep slope at $\Delta_s = 0$ for $\beta = 0$ (the black curve in Fig. 3(a)), which combines the lorentz peak at $\Delta_s = 0$ in Fig. 2, leading to the fast light effect. However, if $\beta \neq 0$, the dispersion will exhibit the positive steep slope at $\Delta_s = 0$, which combines the zero absorption at $\Delta_s = 0$ in Fig. 2, resulting in the slow light effect. It is analogous to EIT[43] in Λ-type atoms systems, a transparency window will lead to the slow light effect, in our system the MF-QD coupling also results in the analogous zero absorption transparency window, which is accompanied with the rapid normal phase dispersion, indicating the coherent optical propagation, such as the fast and slow light effect. No matter what regimes result in the zero absorption, when a transparency window is observed, the slow light or fast light will be induced. In our hybrid coupled QD-SNW/SC system, when the transparency appears in the absorption spectrum, the slope around transparency window of the dispersion will experience the conversion between the negative to positive. The positive steep slope of dispersion will induce the positive group velocity index, i.e., $n_g > 0$, then the slow light phenomenon will appear in the system. On the contrary, if the dispersion shows the negative steep slope, the group velocity index will be negative, i.e., $n_g < 0$, as a result the fast light will be achieved. In Fig. 3(b), we plot the group velocity index n_g of probe laser versus QD-MF coupling strength β under the condition of $\Delta_M = 0$ and $\Delta_p = 0$. We can find that the group velocity index n_g experiences the positive–negative–positive change, which corresponds to the slow-fast-slow light. In Fig. 3(c), we also give the group velocity index n_g as a function of Rabi frequency Ω_p^2 in the case of $\beta = 0$. As the dispersion shows a negative steep slope at $\Delta_s = 0$ for $\beta = 0$ as shown in the black curve in Fig. 3(a), which combines a lorentz peak in Fig. 2 resulting in the fast light effect. Furthermore, the group velocity index n_g varies significantly around $\Omega_p^2 = 0.1\ (\mathrm{GHz})^2$. In Fig. 3(d), we consider the case of $\beta \neq 0$, due to the fact that the dispersion exhibits the positive steep slope at $\Delta_s = 0$, and then the group velocity index n_g is positive with varying the Rabi frequency Ω_p^2, therefore, the slow light effect can be obtained.

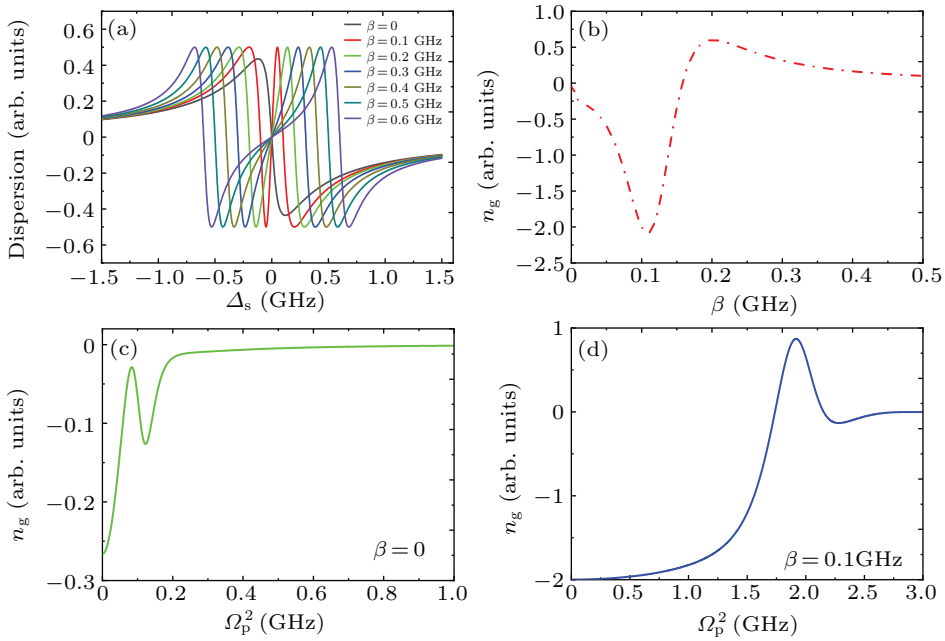


Fig. 3. (a) The dispersion as a function of Δ_s for several different MF-QD coupling strengths β at $\Delta_M = \Delta_p = 0$. (b) The group velocity index n_g versus QD-MF coupling strength β under the condition of $\Delta_M = 0$ and $\Delta_p = 0$. (c) n_g as a function of Ω_p^2 for $\beta = 0$. (d) n_g versus Ω_p^2 for $\beta = 0.1$ GHz.

Secondly, we consider the coupled Majorana edge state, i.e., $\varepsilon_M \neq 0$ (or $\Delta_M \neq 0$) still in the case of $\Delta_p = 0$. In Fig. 4, we display the probe absorption spectra versus Δ_s for different Δ_M, which experience the conversion from unsymmetrical splitting (Fano resonance like splitting) to symmetric splitting (EIT like splitting) to Fano resonance. Unlike EIT with symmetric splitting, the Fano resonance-like splitting is an asymmetry shape due to the fact that the scattering of light amplitude under the condition of EIT is not met and a detuning is introduced. Obviously, the absorption spectra show the Fano-resonance-like splitting under $\Delta_M \neq 0$ due to the MF-QD interaction, and the Fano-like resonance will change into a symmetric EIT-like splitting at $\Delta_M = 0$. Furthermore, the evolution process of the two sharp unsymmetrical peaks varies significantly for different detuning Δ_M, and the amplitude intensity of the left peaks is enhanced and the right peaks are reduced with changing Δ_M from $\Delta_M = -0.3$ GHz to $\Delta_M = 0.3$ GHz. In addition, we find that the absorption spectra are asymmetric

and a prominent avoided crossing phenomenon occurs in the system,[44] which is very different from the case of $\Delta_M = 0$ in Fig. 2, where the absorption spectra split into a doublet with symmetrical splitting and each peak has equal strength. This behavior is attributed to the off-resonant coupling between the QD and MF.

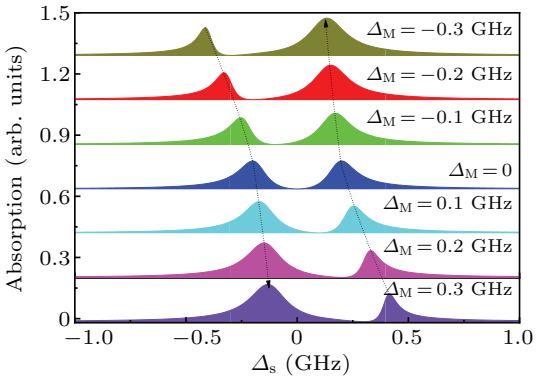


Fig. 4. The probe absorption spectra versus Δ_s for several different Δ_M at the parameters of $\Omega_p^2 = 0.005$ (GHz)^2 and $\beta = 0.1$ GHz.

Therefore, in Fig. 5, we further investigate the slow and fast light effect under the condition of the coupled Majorana edge state ($\Delta_M \neq 0$) for the case of $\Delta_p = 0$. In Fig. 5(a), we plot the absorption and dispersion spectra for the fixed QD-MF coupling strength $\beta = 0.1$ GHz and the Rabi frequency $\Omega_p^2 = 0.005$ (GHz)^2 under $\Delta_M = -0.1$ GHz, and the absorption shows a Fano resonance and the steep slope around $\Delta_s = 0$ in the dispersion changes significantly. Thus, in Fig. 5(b), we further display the dispersion versus Δ_s for several different Δ_M, and the processes of evolutions of the dispersion are related to the coupled Majorana edge state. Here, we only consider the case of $\Delta_M \leq 0$. Figure 5(c) shows the group velocity index n_g as a function of QD-MF coupling strength β under several different Δ_M, and it is obvious that n_g can realize the conversion from fast to slow light. Comparing the condition of $\Delta_M = 0$ with $\Delta_M \neq 0$, we can see that the experience of the group velocity index n_g in $\Delta_M = 0$ is salient from the condition of $\Delta_M \neq 0$. Because the parameter β can be manipulated with controlling the distance between the QD and SNW/SC device, we can obtain fast-to-slow light (or vice versa) by controlling the parameter β in the system. In Fig. 5(d), we also present the group velocity index n_g versus Ω_p^2 for three Δ_M. We obtain that n_g experiences the conversion from slow to fast to slow light at $\Delta_M = -0.1$ GHz. However, if $\Delta_M < -0.1$ GHz (such as $\Delta_M = -0.2$ GHz or -0.3 GHz), the fast light effect will dominate.

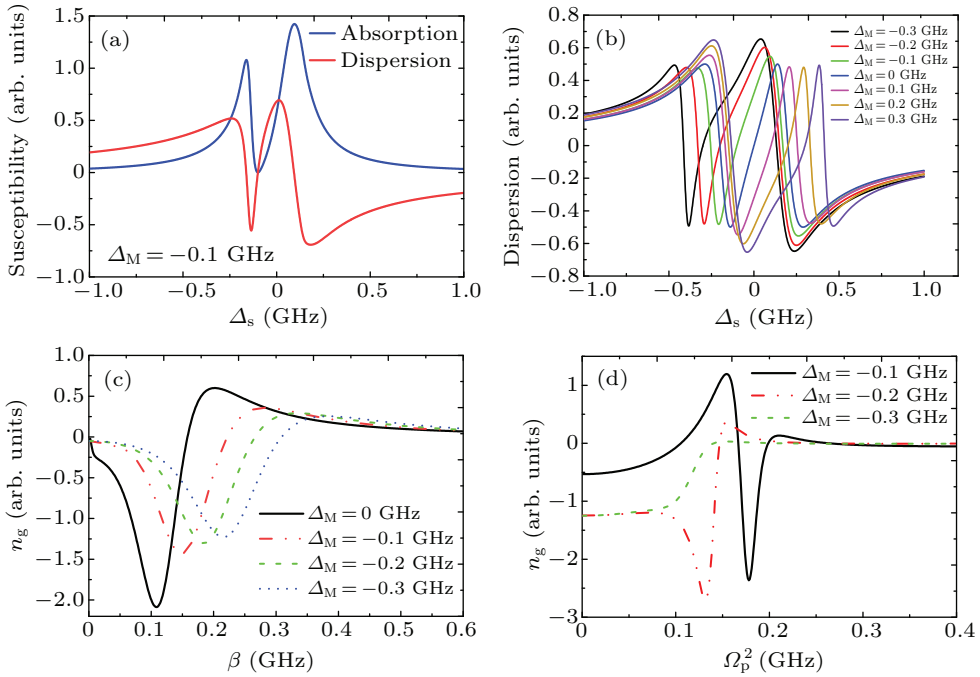


Fig. 5. (a) The absorption and dispersion versus Δ_s at $\Delta_M = -0.1$ GHz. (b) The dispersion versus Δ_s for several different Δ_M at $\Delta_p = 0$. (c) The group velocity index n_g versus β for several different Δ_M. (d) The group velocity index n_g versus Ω_p^2 for several different Δ_M.

In the above discussions, we only consider the case of the exciton-pump field detuning $\Delta_p = 0$, while under the condition of $\Delta_p \neq 0$, the Fano resonance will be altered tempestuously. In Fig. 6(a), we plot the absorption spectra versus Δ_s with increasing Δ_p from $\Delta_p = -0.3$ GHz to $\Delta_p = 0.3$ GHz under the parameters of $\Omega_p^2 = 0.005$ (GHz)^2 and $\beta = 0.2$ GHz in the uncoupled Majorana edge state ($\Delta_M = 0$), which experiences the conversion from Fano resonance to Rabi-like splitting to Fano resonance. Furthermore, besides $\Delta_p = 0$, we find that the peaks in the absorption spectra present mirror symmetry at $\Delta_p = \pm\Theta$ (Θ indicates the definite numerical value) in the uncoupled Majorana edge state. Here, we take $\Delta_p = -0.3$ GHz and $\Delta_p = 0.3$ GHz as an example. If $\Delta_p = -0.3$ GHz, in the absorption spectrum as shown by the red curve in Fig. 6(a),

the left peak locates at $\Delta_s = -0.4$ GHz and the right peak locates at $\Delta_s = 0.1$ GHz. However, if $\Delta_p = 0.3$ GHz, in the absorption spectrum as shown by the purple curve in Fig. 6(a), the left peak locates at $\Delta_s = -0.1$ GHz and the right peak locates at $\Delta_s = 0.4$ GHz. It is obvious that the left peak at $\Delta_p = -0.3$ GHz is mirror symmetric with the right peak at $\Delta_p = 0.3$ GHz, and the right peak at $\Delta_p = -0.3$ GHz is mirror symmetric with the left peak at $\Delta_p = 0.3$ GHz in the absorption spectra. When we change the condition of $\Delta_M = 0$ into $\Delta_M \neq 0$, the Fano resonance manifests evident distinction compared with $\Delta_M = 0$ with varying Δ_p from $\Delta_p = -0.3$ GHz to $\Delta_p = 0.3$ GHz as shown in Fig. 6(b). We find that, with increasing Δ_p from $\Delta_p = -0.3$ GHz to $\Delta_p = 0$, the splitting width of the two peaks in the absorption spectra is reduced, i.e., the absorption spectra is squeezed. However, with increasing Δ_p from $\Delta_p = 0$ to $\Delta_p = 0.3$ GHz, the splitting width of the two peaks in the absorption spectra is enhanced, i.e., the absorption spectra is stretched. No matter whether $\Delta_M = 0$ or $\Delta_M \neq 0$, we obtain that the full width at half maximum (FWHM) of the left peak is reduced and the FWHM of the right peak is enhanced in the absorption spectra with increasing Δ_p from $\Delta_p = -0.3$ GHz to $\Delta_p = 0.3$ GHz as shown in Figs. 6(a) and 6(b).

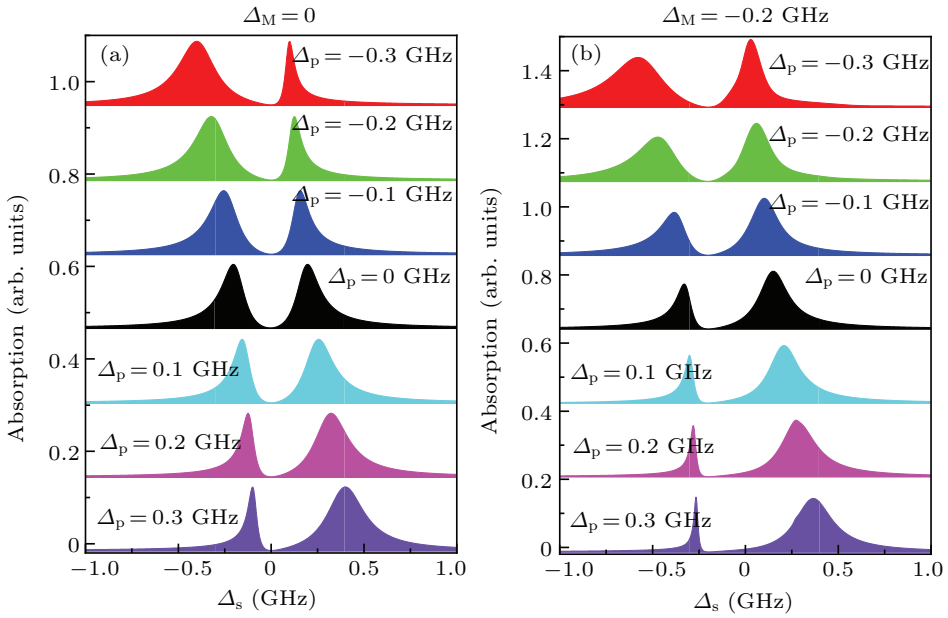


Fig. 6. The absorption spectra versus Δ_s for several different Δ_p at $\Delta_M = 0$. (b) The absorption spectra versus Δ_s for several different Δ_p at $\Delta_M \neq 0$. The other parameters are $\Omega_p^2 = 0.005$ (GHz)^2 and $\beta = 0.2$ GHz.

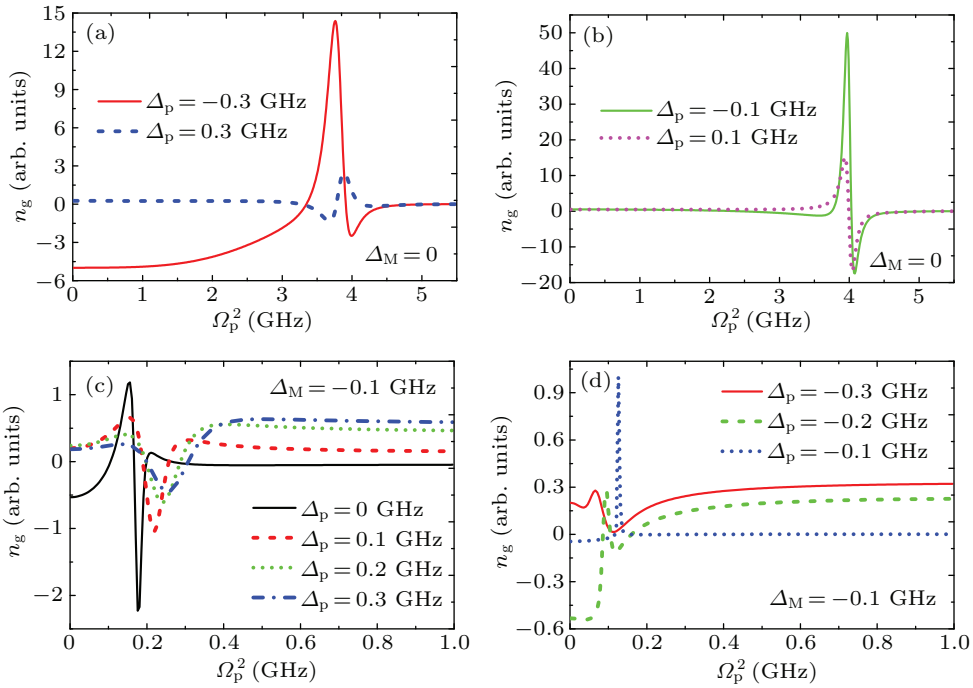


Fig. 7. (a) and (b) The group velocity index n_g versus Ω_p^2 for several Δ_p at $\Delta_M = 0$ and $\beta = 0.2$ GHz. (c) and (d) The group velocity index n_g versus Ω_p^2 for several Δ_p at $\Delta_M \neq 0$ and $\beta = 0.2$ GHz.

Then, on the other hand, we also demonstrate the coherent optical propagation properties for different $\Delta_p \neq 0$ and $\Delta_M \neq 0$. In Fig. 7(a), we investigate the group velocity index n_g as a function of Ω_p^2 for $\Delta_p = -0.3$ GHz and $\Delta_p = 0.3$ GHz under $\Delta_M = 0$ at fixed $\beta = 0.2$ GHz. Figure 7(b) gives n_g versus Ω_p^2 for $\Delta_p = -0.1$ GHz and $\Delta_p = 0.1$ GHz under $\Delta_M = 0$ at fixed $\beta = 0.2$ GHz. Compared Fig. 7(a) with Fig. 7(b) corresponding to Fig. 6(a), we find that the group velocity index n_g undergoes the conversion from advance to delay which corresponds to fast to slow light, and the conversion is more remarkable at $\Delta_p < 0$ than at $\Delta_p > 0$. In Fig. 7(c), we give n_g versus Ω_p^2 at $\Delta_M \neq 0$ with increasing Δ_p from $\Delta_p = 0$ to $\Delta_p = 0.3$ GHz, and Fig. 7(d) plots n_g versus Ω_p^2 at $\Delta_M = -0.1$ GHz for $\Delta_p < 0$, which corresponds to Fig. 6(b). We can obtain that the conversion from fast to slow light can reach in the two conditions, and compared with Fig. 7(c), the process of evolution of the conversion from fast to slow light is slightly different from Fig. 7(d). Thus, with controlling different detuning regimes, the fast-to-slow light, or vice versa, can be reached in our system.

In our system, we only consider the QD coupling to the nearby MFs, i.e., QD only couples to one MF due to the fact that it is confined by the length of the SNW and the superconducting coherent length. If QD is coupled to a pair of MFs, the results are significantly different. We have ever designed a hybrid QD-SNW/SC ring device, where QD is coupled to a pair of MFs,[34,35] and the results indicate that both the absorption spectra and the slow light (fast light) are enhanced observably compared with the results in this paper. In order to enhance the coherent optical properties (such as the linear or nonlinear optical phenomena) of QD induced by MFs, we have ever considered introducing a hybrid QD-nanoresonator system to investigate MFs induced coherent optical phenomena,[32,33] and the results manifest that both the linear or nonlinear optical phenomena induced by MFs are enhanced significantly due to the fact that the nanoresonator behaves as a phononic cavity, which enhances the linear and nonlinear optical effect. Therefore, to reach enhanced fast and slow light effect, the hybrid QD-nanoresonator system can be brought, and we will investigate the issue in the future work.

4. Conclusions

In summary, we have demonstrated the coherent optical propagation properties in a hybrid QD-SWN/SC device, which includes a QD driven by a pump field and a probe field coupled to a nearby MF in the hybrid SWN/SC system, and we investigate the absorption spectra of the probe field under both the conditions of the pump on-resonance ($\Delta_p = 0$) and off-resonance ($\Delta_p \neq 0$). In the situation of pump on-resonance, the absorption spectra displays a Rabi-like splitting manifesting the strong interaction between the QD and MF. In pump off-resonance, the absorption spectrum experiences the conversion from Fano resonance to Rabi-like splitting in different parametric regimes. Moreover, the narrow transparency window (i.e., the absorption dip approaches zero) in the absorption spectrum and the corresponding rapid phase dispersion allow for reaching the slow light effect. The results show that the group velocity index can be controlled by the QD-MF coupling, which can reach the conversion from fast to slow light.

Acknowledgements

This work was supported by the National Natural Science Foundation of China (Grant Nos. 11804004 and 11647001), the China Postdoctoral Science Foundation (Grant No. 2020M681973), and Anhui Provincial Natural Science Foundation, China (Grant No. 1708085QA11).

References

[1] Elliott S R and Franz M 2015 *Rev. Mod. Phys.* **87** 137
[2] Zhou K, Zhang C, Qin L and Li X Q 2021 *Chin. Phys. B* **30** 010301
[3] Gong W J, Xue Y H, Wang X Q, Zhang L L and Yi G Y 2021 *Chin. Phys. B* **30** 077307
[4] Liu J, Li K M, Chi F, Fu Z G, Hou Y F, Wang Z and Zhang P 2020 *Chin. Phys. B* **29** 077302
[5] Chen L, Zhang Y Q and Han R S 2018 *Chin. Phys. B* **27** 077102
[6] Deng M X, Zheng S H, Yang M, Hu L B and Wang R Q 2015 *Chin. Phys. B* **24** 037302
[7] Shang E M, Pang Y M, Shao L B and Wang B G 2014 *Chin. Phys. B* **23** 057201
[8] Alicea J 2012 *Rep. Prog. Phys.* **75** 076501
[9] Mourik V, Zuo K, Frolov S M, Plissard S R, Bakkers E P and Kouwenhoven L P 2012 *Science* **336** 1003
[10] Das A, Ronen Y, Most Y, Oreg Y, Heiblum M and Shtrikman H 2012 *Nat. Phys.* **8** 887
[11] Deng M T, Yu C L, Huang G Y, Larsson M, Caroff P and Xu H Q 2012 *Nano Lett.* **12** 6414
[12] Chen J, Yu P, Stenger J, Hocevar M, Car D, Plissard S R, Bakkers E P A M, Stanescu T D and Frolov S M 2017 *Sci. Adv.* **3** e1701476
[13] Nadj-Perge S, Drozdov I K, Li J, Chen H, Jeon S, Seo J, MacDonald A H, Bernevig B A and Yazdani A 2014 *Science* **346** 602
[14] Yin J X, Wu Z, Wang J H, Ye Z Y, Gong J, Hou X Y, Shan L, Li A, Liang X L, Wu X X, Li J, Ting C S, Wang Z Q, Hu J P, Hor P H, Ding H and Pan S H 2015 *Nat. Phys.* **11** 543
[15] Albrecht S M, Higginbotham A P, Madsen M, Kuemmeth F, Jespersen T S, Nygård J, Krogstrup P and Marcus C M 2016 *Nature* **531** 206
[16] Sun H H, Zhang K W, Hu L H, Li C, Wang G Y, Ma H Y, Xu Z A, Gao C L, Guan D D, Li Y Y, Liu C, Qian D, Zhou Y, Fu L, Li S C, Zhang F C and Jia J F 2016 *Phys. Rev. Lett.* **116** 257003
[17] He Q L, Pan L, Stern A L, Burks E C, Che X, Yin G, Wang J, Lian B, Zhou Q, Choi E S, Murata K, Kou1 X, Chen Z, Nie T, Shao T Q, Fan Y, Zhang S C, Liu K, Xia J and Wang K L 2017 *Science* **357** 294
[18] Rokhinson L P, Liu X and Furdyna J K 2012 *Nat. Phys.* **8** 795
[19] Jeon S, Xie Y, Li J, Wang Z, Bernevig B A and Yazdani A 2017 *Science* **358** 772
[20] Urbaszek B, Marie X, Amand T, Krebs O, Voisin P, Maletinsky P, Högele A and Imamoglu A 2013 *Rev. Mod. Phys.* **85** 79
[21] Yang S, Dou X M, Yu Y, Ni H Q, Niu Z C, Jiang D S and Sun B Q 2015 *Chin. Phys. Lett.* **32** 077804
[22] Qin L G and Wang Q 2017 *Chin. Phys. Lett.* **34** 017303
[23] Tang J and Xu X L 2018 *Chin. Phys. B* **27** 027804
[24] Gu Y, Tang L B, Guo X P, Xiang J Z, Teng K S and Liu S P 2019 *Chin. Phys. B* **28** 047803
[25] Li S, Shi L and Yan Z W 2020 *Chin. Phys. B* **29** 097802

[26] Liu D E and Baranger H U 2011 *Phys. Rev. B* **84** 201308

[27] Flensberg K 2011 *Phys. Rev. Lett.* **106** 090503

[28] Leijnse M and Flensberg K 2011 *Phys. Rev. B* **84** 140501

[29] Pientka F, Kells G, Romito A, Brouwer P W and von Oppen F 2012 *Phys. Rev. Lett.* **109** 227006

[30] Sau J D and Sarma S D 2012 *Nat. Commun.* **3** 964

[31] Deng M T, Vaitiekėnas S, Hansen E B, Danon J, Leijnse M, Flensberg K, Nygård J, Krogstrup P and Marcus C M 2016 *Science* **354** 1557

[32] Chen H J and Zhu K D 2014 *Nanoscale Res. Lett.* **9** 166

[33] Chen H J, Fang X W, Chen C Z, Li Y and Tang X D 2016 *Sci. Rep.* **6** 36600

[34] Chen H J and Wu H W 2018 *Sci. Rep.* **8** 17677

[35] Chen H J 2020 *Quantum Inf. Process.* **19** 171

[36] Ridolfo A, D Stefano, O, Fina N, Saija R and Savasta S 2010 *Phys. Rev. Lett.* **105** 263601

[37] Agarwal G S and Huang S 2010 *Phys. Rev. A* **81** 041803

[38] Boyd R W 1992 *Nonlinear Optics* (San Diego: Academic) p. 225

[39] Harris S E, Field J E and Kasapi A 1992 *Phys. Rev. A* **46** R29

[40] Bennink R S, Boyd R W, Stroud C R and Wong V 2001 *Phys. Rev. A* **63** 033804

[41] Boyd R W and Gauthier D J 2009 *Science* **326** 1074

[42] Wilson-Rae I, Zoller P and Imamoglu A 2004 *Phys. Rev. Lett.* **92** 075507

[43] Fleischhauer M, Imamoglu A and Marangos J P 2005 *Rev. Mod. Phys.* **77** 633

[44] Liu Y C, Luan X, Li H K, Gong Q, Wong C W and Xiao Y F 2014 *Phys. Rev. Lett.* **112** 213602